Fluid Mechanics
2021; 7(2): 17-28
http://www.sciencepublishinggroup.com/j/fm
doi: 10.11648/j.fm.20210702.11
ISSN: 2575-1808 (Print); ISSN: 2575-1816 (Online)

An Integrated Approach to Predict Wind Resource Energy from an Urban Wind Turbine in a Complex Built Environment

Neihad Hussen Al-Khalidy

CFD, Wind & Energy Technical Discipline, SLR Consulting, Sydney, Australia

Email address:
Nal-khalidy@slrconsulting.com

To cite this article:
Neihad Hussen Al-Khalidy. An Integrated Approach to Predict Wind Resource Energy from an Urban Wind Turbine in a Complex Built Environment. *Fluid Mechanics*. Vol. 7, No. 2, 2021, pp. 17-28. doi: 10.11648/j.fm.20210702.11

Received: June 30, 2021; **Accepted**: July 15, 2021; **Published**: July 27, 2021

Abstract: Introducing an urban wind turbine in the crowded and complex City of North Sydney built environment can provide a significant opportunity to generate onsite wind energy and reduce electric demand and utility costs. Elevated turbulent conditions present a number of well-known challenges to urban wind turbines and as a result the energy production may reduce due to changes in wind speeds and directions. This current case study presents a procedure to optimize urban wind turbine energy production comprising key steps which include the project site potential for the installation of wind turbines, the estimation of the annual wind power available and the cost estimate for installation and maintenance. The wind potential for the project site was initially determined from statistical wind data cross-referenced with typical weather data for the Sydney region. Computational Fluid Dynamics (CFD) simulations of principal wind directions were then used to adjust the local wind climate data and establish a suitable wind turbine position. Finally, the annual energy production for a number of 10-20 kW commercially available wind turbines was estimated taking into account the wind turbine power curve and technical specifications. The CFD simulations in the current study accounted for the complex site topography and incorporated the shielding impact of nearby trees and other vegetation in order to find the least turbulent area for a successful installation. This study assessed all the parameters that have impact on the accuracy of the numerical model including, computational domain, mesh distribution, numerical scheme and CFD results integration with the localized weather data for the project site.

Keywords: CFD, Urban Wind Energy, Urban Wind Turbines, Complex Terrain, Tree Modelling

1. Introduction

Growing the clean energy sector will be necessary to divest from fossil fuels, drive innovations and achieve the 2015 Paris climate change goals. Among various renewable energy resources, Urban Wind Turbines (UWTs) can be a significant source for generating wind energy. Government financial incentives are in place for small wind turbines in many countries. Small wind systems can also generate Renewable Energy Certificates (RECs). There are two types of urban wind turbines:

1) Horizontal axis wind turbines in which the main rotor shaft is pointed in the direction of the wind to extract power. Horizontal wind turbines work well when the air flow is less turbulent.
2) Vertical axis wind turbines in which the main rotor shaft is set transverse to the wind. Vertical wind turbines are known to be less efficient than horizontal wind turbine due to design and operational characteristic issues.

Several guidelines for UWTs in the built environment have been provided (such as [1-3]). These guidelines help the deployment of UWTs in the built environment.

Permit approval of urban wind turbines requires the following key considerations:

1) The UWT should supply the required energy.
2) The UWT should be quiet.
3) Shadows should be minimised, with less bulky systems preferred.
4) The UWT must not generate vibration.
5) A planning permit will typically be required if the system is visible from a street [3].

In comparison to rural wind turbines, UWTs are

characterized by lower annual wind speed, more frequent changes in wind directions and increased turbulence due to the presence of buildings, obstacles and landscape features. UWTs may therefore not generate the expected energy if the location is not appropriately selected.

To date, most wind turbines installed in the built environment have been sited with limited understanding of the unique challenges of UWTs [4].

The urban wind turbines industry is evolving rapidly, and a roadmap has been provided to overcome the identified barriers and outline short and medium-term stakeholder actions [5].

To achieve a successful deployment, wind turbines must be installed in areas where the wind speed is high and the turbulence as low as possible. Various techniques are used for site identification of UWTs. These include:

1) Site measurements including a wind mast for at least 3 months, ideally 12 months, to obtain localised wind data ([6, 7]).
2) Simplified analytical models for the wake deficit ([5, 8]) which depends on the thrust and rotor diameter of the turbine and an empirical wake expansion coefficient. Commercial software for layout optimization, e.g. WindPro [9] and Openwind [10] use analytical models including empirical wake expansion coefficients.
3) Wind Tunnel Testing [i.e. 11].
4) Numerical techniques such as Computational Fluid Dynamics (CFD) modelling.

A considerable number of CFD publications for the assessment of windflow around buildings in complex-built environments have been published in the in the past two decades [such as [12-16]). The CFD method allows for providing comprehensive output (velocity distribution in three dimensions, pressure profile, turbulence levels) and enables layout optimization.

A literature review of CFD simulations of the wind flow around buildings for urban wind energy applications is provided in [17]. A significant number of the CFD references use CFD to predict localized wind flow, discussing the turbulence modelling, numerical schemes, meshing and the best practice guidelines used for the CFD simulation of the urban wind for wind energy exploitation purposes.

Several studies have carried out comparisons between CFD simulations and field measurements to evaluate the wind resources available in a real urban area (such as [18-21]). Resendable agreements were achieved using the realizable k-epsilon (k-ε) model.

The current study provide an integrated approach to predict the wind resource energy for the entire project site from localized statistical wind data cross-referenced with the CFD (Computational Fluid Dynamics) simulation results to establish a suitable wind turbine position and detailed energy data at the preferred wind turbine locations.

The main elements of this case study are:

1) Analyse the local weather data and develop a statistical wind climate model for the project site.
2) Utilise 3D CFD modelling tools to assess the potential for the installation of wind turbines at the site.
3) Adjust the previously developed statistical wind climate based on the CFD results at the proposed wind turbine locations.
4) Estimate the annual wind power for selected commercial wind turbines.
5) Optimize energy production where possible and required.

2. Fundamental Flow Equations

The CFD model solves the continuity and momentum and energy (if required) equations as required. The equations for a steady state case can be written as follows:

$$\frac{\partial}{\partial x_i}(\rho u_i) = 0$$

$$\frac{\partial}{\partial x_j}(\rho u_i u_j) = -\frac{\partial p}{\partial x_i} + \frac{\partial \tau_{ij}}{\partial x_j}) + \rho g_i + F_i$$

$$\frac{\partial}{\partial x_i}(\rho h) + \frac{\partial}{\partial x_i}(u_i \rho h) = \frac{\partial}{\partial x_i}(k_{effective} \frac{\partial T}{\partial x_i}) + S$$

Where ρ is the density of air, u is the air velocity, p is the static pressure, ρg and F are the gravitational body and external body forces, τij is the stress tensor, h is the enthalpy, $k_{effective}$ is the effective thermal conductivity and S is the volumetric heat source.

Turbulence is described by the Navier Stokes equations and modelled in the current study using a Realizable k-ε turbulence model [22].

3. Case Study

3.1. Project Description

The project site (Refer Figure 1) has been transformed from an ex-industrial site in North Sydney to regenerated waterfront parklands including community gardens, food gardens, a native bush nursery and public spaces.

Figure 1. *Project Site.*

3.2. Local Weather Data

The data of interest in this study are the annual mean hourly wind speeds experienced throughout the year, how these winds vary with azimuth, and the seasonal break-up of winds into the primary Sydney wind seasons.

In relation to key characteristics of the Sydney Region Wind Climate, Sydney is affected by two primary wind seasons:

1) Summer winds occur mainly from the northeast, southeast and south. While northeast winds are the more common prevailing wind direction (occurring typically as offshore land-sea breezes), southeast and south winds generally provide the strongest gusts during summer.
2) Winter/Early spring winds occur mainly from the west and the south. West quadrant winds (southwest to northwest) provide the strongest winds during winter and in fact for the whole year.

The probability for different wind events for Sydney Region is illustrated in Figure 2. The figure simultaneously shows statistical wind data for Sydney region including speed, direction and frequency at RL=10 m for a Typical Meteorological Year (TMY). Note that wind speed increases with height.

The TMY format is one common methodology for creating this dataset and was originally developed for ventilation and energy system simulations. TMY data is not truly-averaged climate data. Rather, it is 12 individual months of selected observational data that is concatenated to form a complete year. The data is selected so that it presents the range of weather conditions for the Sydney region, which are consistent with the long-term averages for the location. It is anticipated that TMY data leads to slightly conservative energy production data for the site when compared to actual weather data.

Figure 2 shows that west quadrant winds (southwest to northwest) provide the strongest winds during winter and in fact for the whole year.

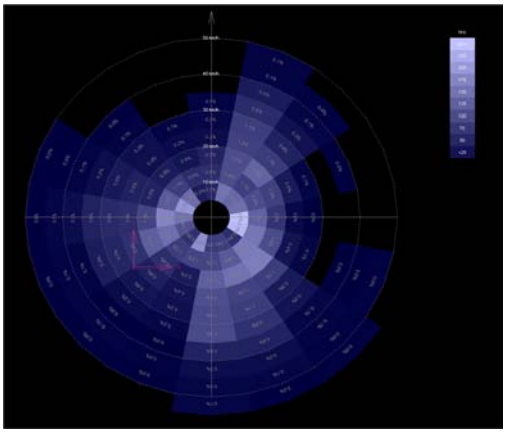

Figure 2. *Sydney TMY Annual Wind Distribution.*

The following conclusions can be reached from Figure 2:

1) Wind speeds are less than 10 km/hr 27.5% of the time
2) 10-20 km/hr occur 42.9% of the time.
3) 20-30 km/hr occur 19.1% of the time.
4) 30-40 km/hr occur 8.63% of the time.
5) 40-50 km/hr occur 1.81% of the time.
6) Wind speeds are higher than 50 km/hr ~0.1% of the time.

Most urban wind turbines are designed to operate at wind speeds around 3.5 m/s (12.6 km/hr). However, higher wind speeds in the order of 5 m/s (18 km/h) are recommended to produce reasonable wind energy for any site, given the "u^3" relationship between wind energy and wind speed.

A proven approach for the development of statistically reliable wind climate information is to express the probability of exceedance of mean winds at a specific location, as the combination of the probability distribution of wind incidence (of any magnitude) by wind direction, and conditional Weibull distributions of wind speed (by wind direction, 0° to 360°):

The wind speed (u) is distributed as the following Weibull distribution assuming a two-parameter distribution where c and k are the scale parameter and the shape parameter, respectively.

$$f(u)=\frac{k}{c}\left(\frac{u}{c}\right)^{k-1}\exp\left[-\left(\frac{u}{c}\right)^{k}\right] \quad (k>0,\ u>0,\ c>1)$$

Figure 3 shows the calculated Weibull parameters for the analysed weather data, determined in 22.5° increment.

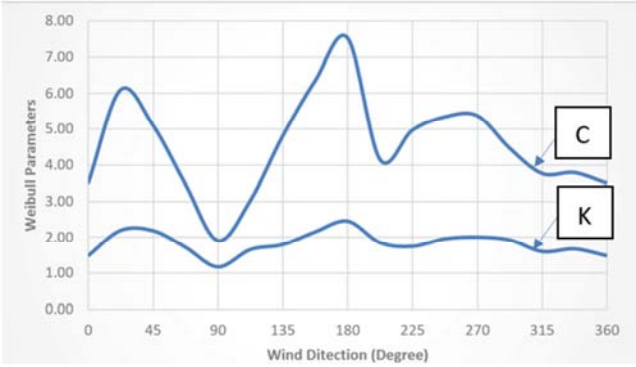

Figure 3. *Weibull Parameters for 22.5° Band.*

3.3. CFD Modelling

3.3.1. Modelling Configuration

A 3D model of the project site, surrounding buildings and structure blocks was created from the supplied drawing and available digital data for the project site.

The 3D Model of the proposed development and surrounding blocks is shown in Figure 4 and Figure 5.

Figure 4. *Geometry for CFD Modelling.*

The project site near-field includes tall, dense trees. Their presence would reduce local wind speeds, especially for east-southeast winds. The impact of trees is included in the

current model utilising special-purpose porous media modelling techniques.

The CFD model accounts for detailed site topography as well as building features as per the provided architectural drawings.

A calculation domain of approximately 2,200 m length, 2,100 m wide and 500 m high was used for the CFD analysis.

Eight key prevailing wind directions were modelled, and wind speeds recorded at the areas of interest.

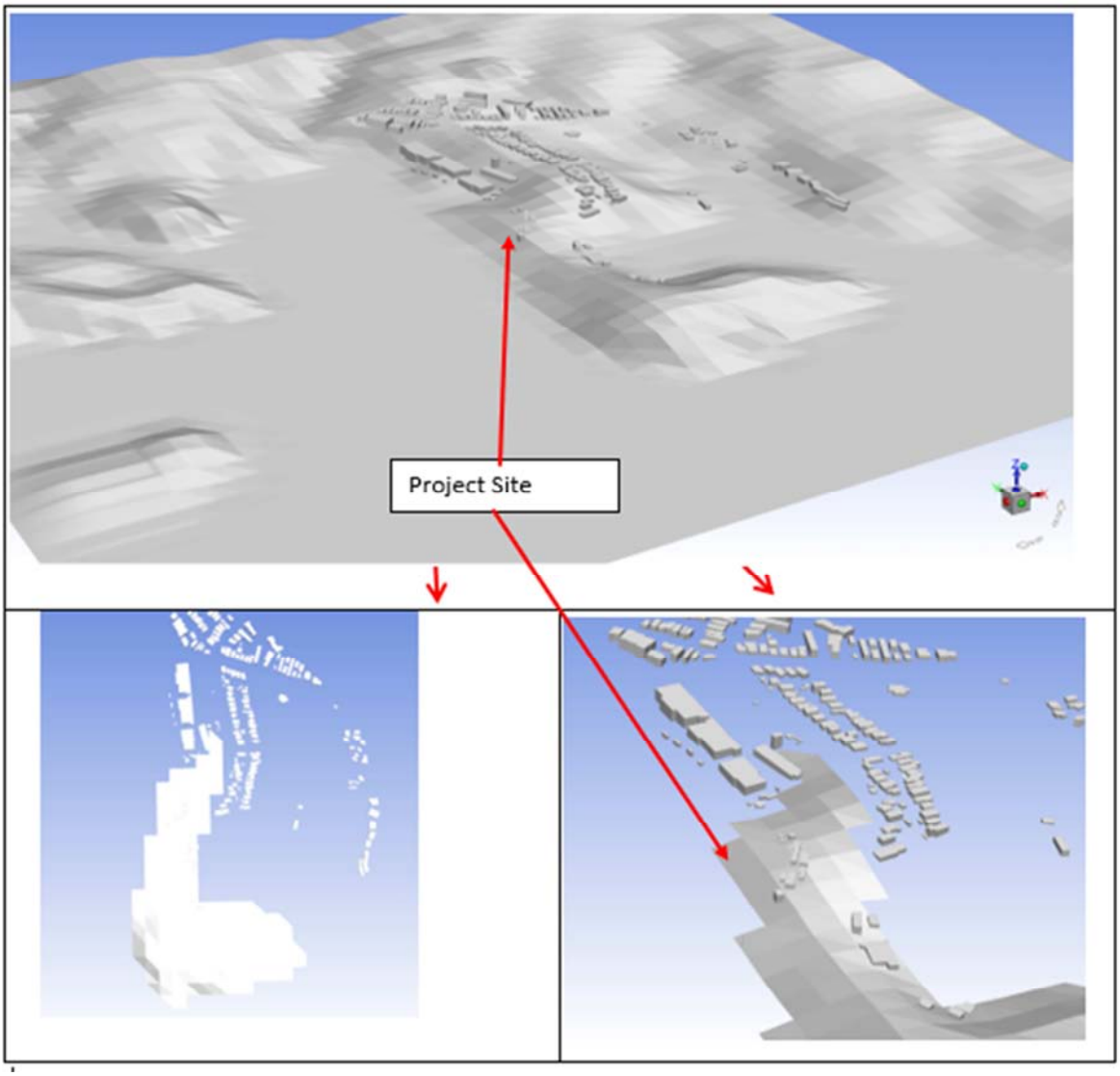

Figure 5. *3D Model for the Project Site.*

3.3.2. Area of Interest

In the CFD modelling, wind speed can be reported at any point on the ground, horizontal and at any vertical elevation. The area of interest for the potential UWT installation is ideally the area with least turbulence.

3.3.3. Sensitivity Analysis

(i) Extent of Built Environment

The size of the computational domain should be selected according to CFD best practice guidelines. A building with height H may have a minimal influence if its distance from the region of interest is greater than 6-10H [17].

All buildings within at least a 450 m diameter were included in the developed CFD model (Refer Figure 3 and Figure 4).

(ii) Top of the Computational Domain

The top of the computational domain should be at least 5H away from the tallest building with height H [17].

To avoid artificial flow over the building, 8.5H is used in this study where H is the building height.

(iii) Mesh Sensitivity Analysis

Based on a mesh sensitivity assessment, 21,529,023 polyhedral cells were used to cover the computational domain. A minor accuracy benefit could be gained if the number of cells was increased to more than 22 million. On the other hand, significant computational time is saved for the 21,529,023 cells scenario.

In general, the grid resolution should be as high as the available computational power permits.

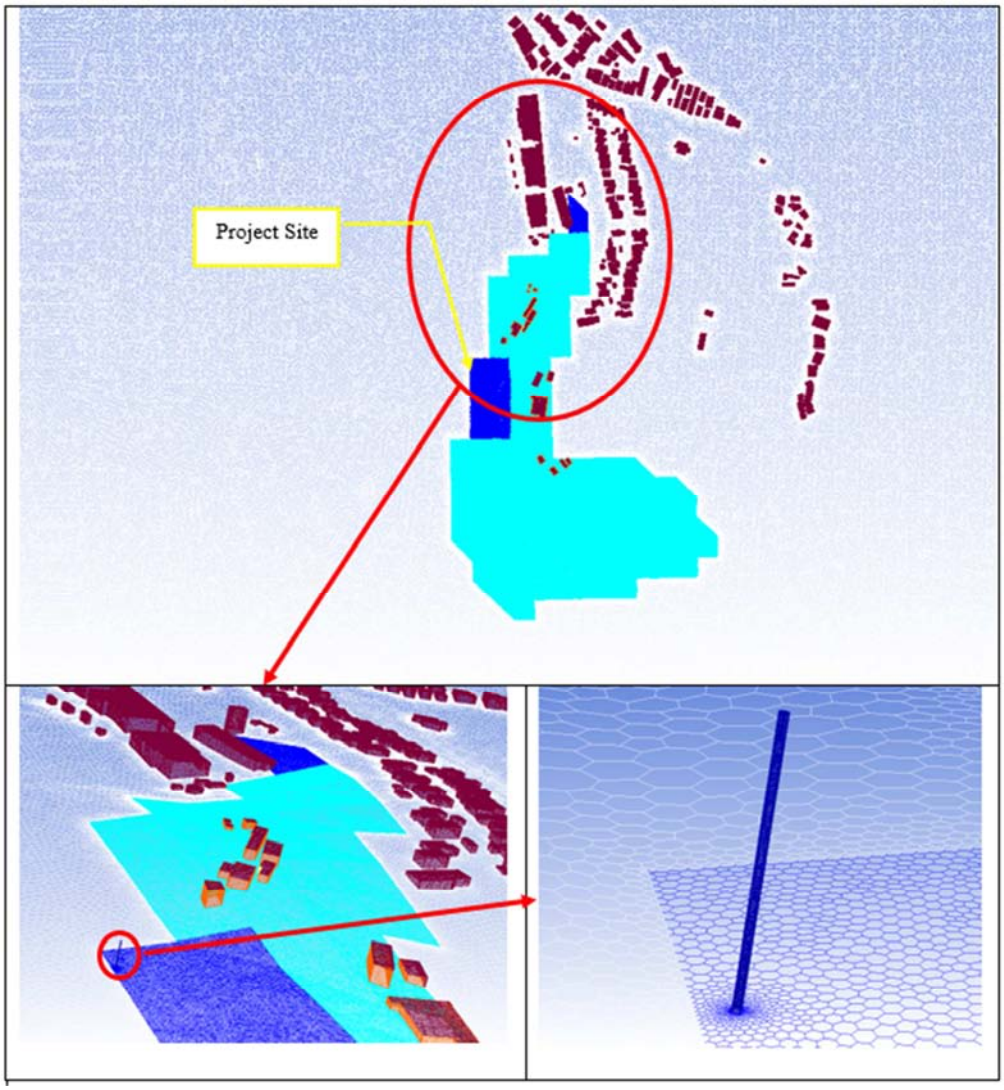

Figure 6. *Mesh Density for the Area of Interest.*

3.3.4. Discretization

The software package utilised in the current CFD analysis is the commercially available code ANSYS- Fluent [22]. The CFD model solves continuity and momentum in the computational domain to predict the airflow at and around the project site.

1) The quality of the mesh is a critical aspect of the overall numerical simulation, and it has a significant impact on the accuracy of the results and solver run time.
2) For the current analysis, polyhedral elements with a total number of 21,529,023 nodes were used to cover the external (outdoor) and the internal (indoor) computational domain. Mesh density is shown in Figure 6. Polyhedral cells are especially beneficial for complex geometries including site topography, can handle recirculating flows and may provide more accurate results than even hexahedra mesh. For a hexahedral cell, there are three optimal flow directions which lead to the maximum accuracy while for a polyhedron with 12 faces there are six optimal directions which, together with the larger number of neighbors, lead to a more accurate solution with a lower cell count [15]. It is also worth mentioning that the development of hexahedral elements for real and complex built environment is challenging.

The following techniques were used for discretization:

1) A second-order numerical scheme for discretization of pressure and momentum to obtain more accurate results.
2) A Realizable k-ε turbulence model was used for all analysed cases due to computational time advantages and model capability to capture flow separation and circulation.
3) The solution was also combined with a standard wall function to avoid using very fine elements near the walls.
4) An iterative procedure was used to estimate the air velocity in terms of three directions, pressure profile and turbulence parameters.

Figure 7 shows that the normalised residuals of continuity for the simulation were reduced by four order of magnitudes while the normalised residuals for x-, y-, and z-velocity, k and epsilon were reduced between six and eight orders of

magnitude demonstrating a valid numerical solution.

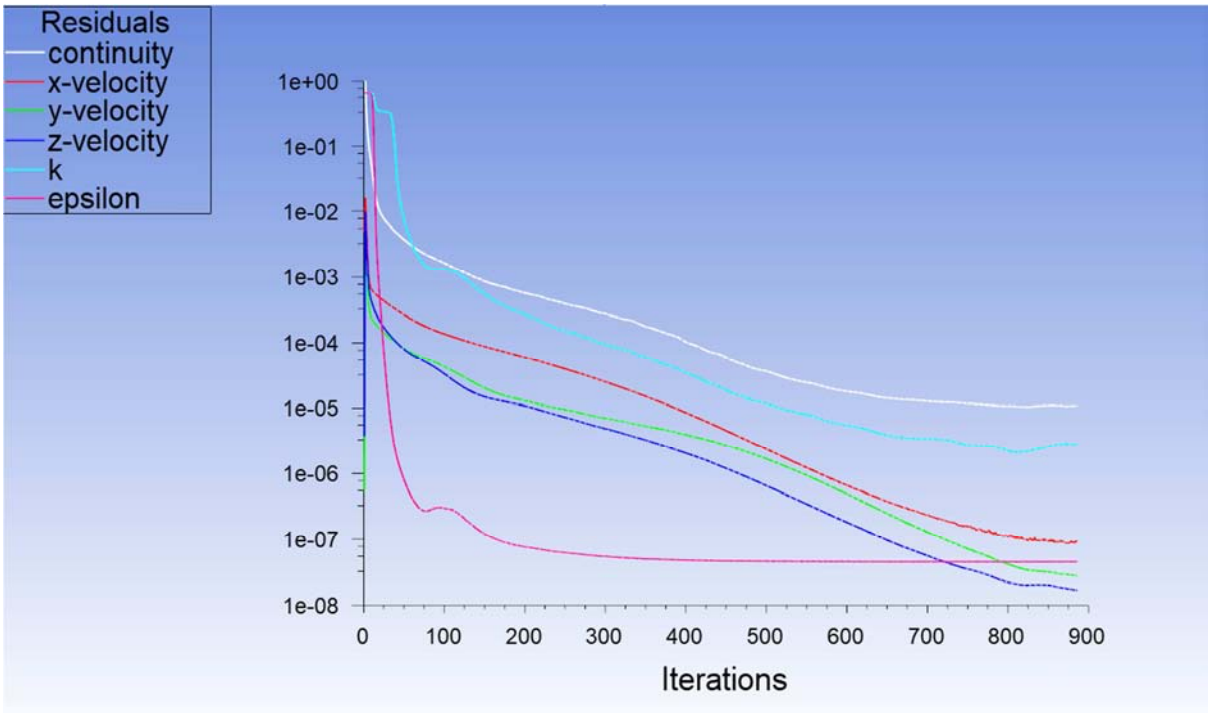

Figure 7. *Scaled Residual History.*

3.3.5. Boundary Conditions

(i) Wind Conditions

The CFD study was undertaken to estimate the local velocity and pressure profile at any potential turbine position of interest. An estimate of average wind velocity was determined for eight prevailing wind conditions, 0° to 360° in 45° increments.

At the upwind free boundary inlet, velocity profiles were derived from weather data combined with adjustment factors found in the Australian Wind Code AS1170.2 based on the Terrain Category for wind directions ranging from 0° to 360°.

At the downwind and upper free boundaries constant pressure boundary conditions were applied.

The following prevailing wind conditions were modelled:

0°	North Winds	45°	Northeast Winds
90°	East Winds	135°	Southeast Winds
180°	South Winds	225°	Southwest Winds
270°	West Winds	315°	Northwest Winds

(ii) Other Boundary Conditions

The following additional boundary conditions were used:

Turbulence quantities (kinetic energy and dissipation rate) were calculated from empirical relationships.

3.4. CFD Results and Discussion

Sample results are presented for 4 wind directions:

3.4.1. North Wind

Figure 8 shows mean velocity ratios ($V_{local}/V_{reference}$ at 10m) through a 2D section at 15 m above the ground. Velocity ratios are plotted on a colour coded scale between 0 and 2.

One can see that the CFD model captures the fluid flow characteristics in significant detail. Wind approaches the site from the north as per the given boundary conditions. Wind is then impacted by the site topography, accelerated near the edges and stagnated and recirculated behind the modelled buildings. The following conclusions can be reached from Figure 8:

1) The development site receives limited immediate shielding at the area of interest.
2) The airflow is accelerated upstream of a proposed mast location due to the favorable localised site topography.
3) A wind speed ratio of 1.3 is observed at the proposed mast location

3.4.2. Northeast Wind

The northeast wind simulation results are presented in Figure 9. The following conclusions can be reached:

1) The development site receives limited shielding and the site is impacted by the cliffs to the northeast.
2) A maximum wind speed ratio of 0.85 is observed at the proposed mast location.

3.4.3. West Wind

The west wind simulation results are presented in Figure 10. The following conclusions can be reached:

1) The development site receives limited shielding and the site impacted by the cliff to the northwest.
2) The highest wind speed ratio is obtained upstream of the project site.
3) An average wind speed ratio of 1.1 is observed at the proposed mast location. The maximum wind speed ratio

at the mast location is 1.25.

3.4.4. Southwest Wind

The southwest wind simulation results are presented in Figure 11. The following conclusions can be reached:

1) The development site receives shielding from the site topography, trees and buildings to the southwest.
2) A maximum wind speed ratio of 0.96 is observed at the proposed mast location.

3.5. Summary CFD Results

Eight different wind directions for the project site area were analysed to determine the local wind velocities in relation to the available wind potential for this North Sydney site. A reference wind speed (V10) was used to calculate the wind speed at a proposed mast location 15 m above the ground elevation at the project site. The ratio between these two wind speeds is shown in Table 1.

Table 1. *Local Wind Speed Ratio at 15m above Ground.*

Wind Direction	Speed-up (v_{local}/v_{10}) at Proposed Mast Location: 15 m above ground
N	1.30
NE	0.85
E	0.85
SE	0.83
S	0.90
SW	0.96
W	1.10
NW	1.34

3.6. Wind Speed Distribution Adjustment

The Weibull parameters (Refer Figure 3) are adjusted for the project site based on results of CFD simulations. The results at a proposed mast location at 15 m above ground is shown in Figure 12.

The localized Weibull parameters including all wind directions are k=1.9 and C=4.5 m/s.

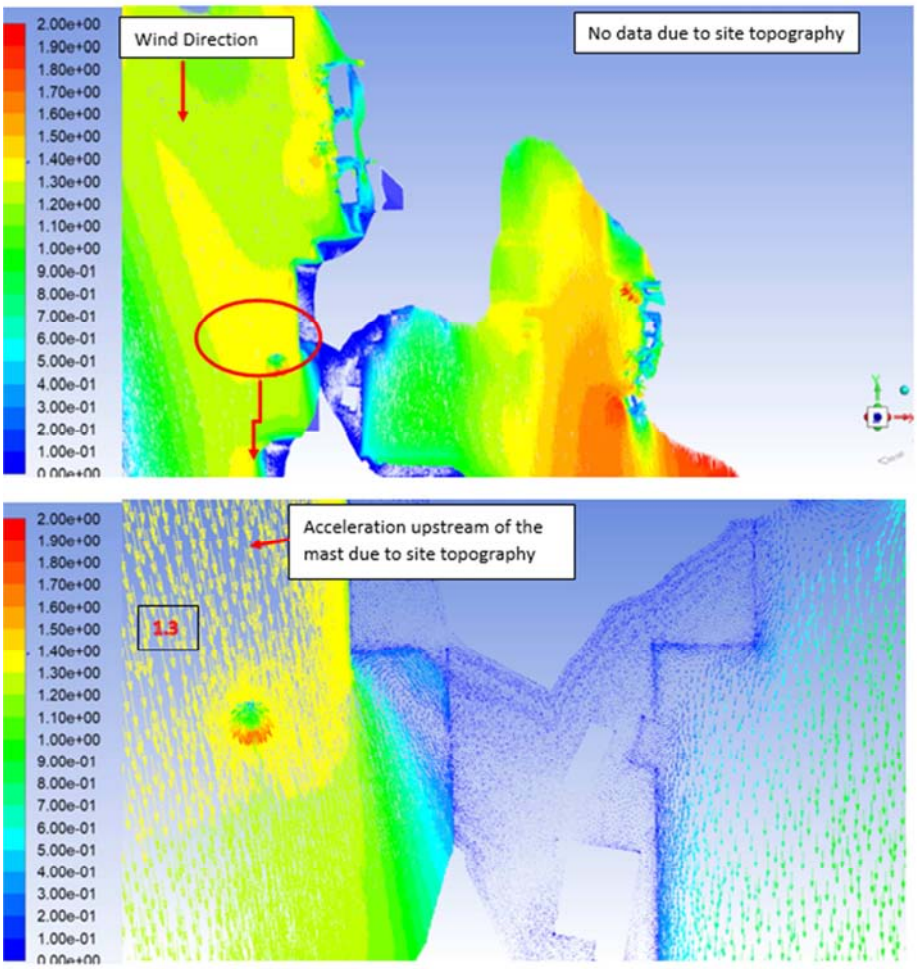

Figure 8. *Mean Velocity Ratios ($V_{local}/V_{reference}$ at 10m) Coloured by Velocity Vector – North Wind (15 m above the ground).*

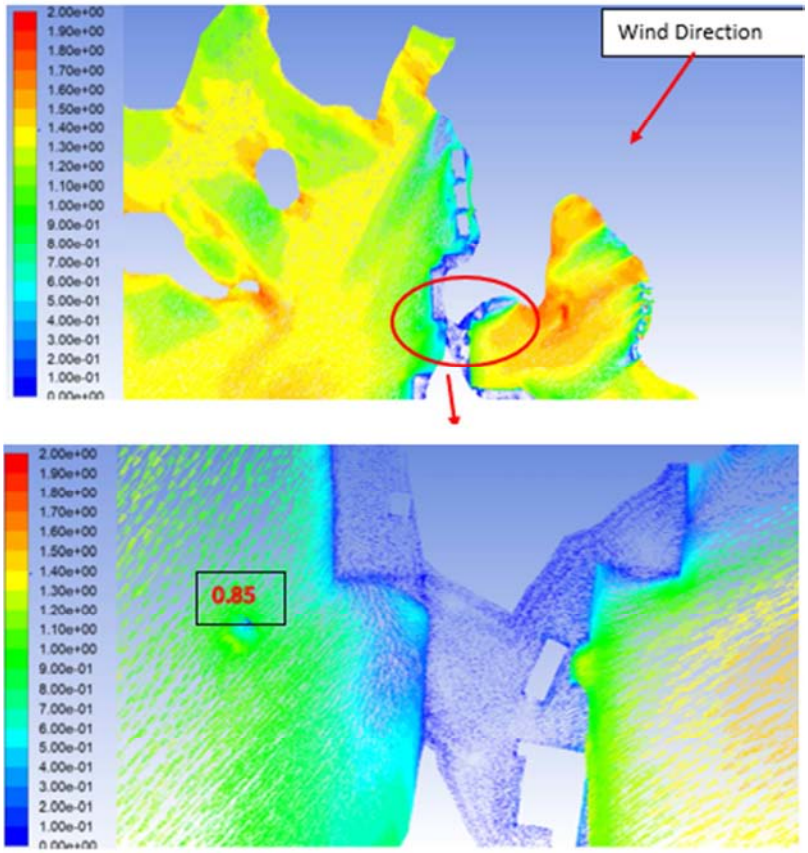

Figure 9. *Mean Velocity Ratios ($V_{local}/V_{reference}$ at 10m) Coloured by Velocity Vector – Northeast Wind (15 m above the ground).*

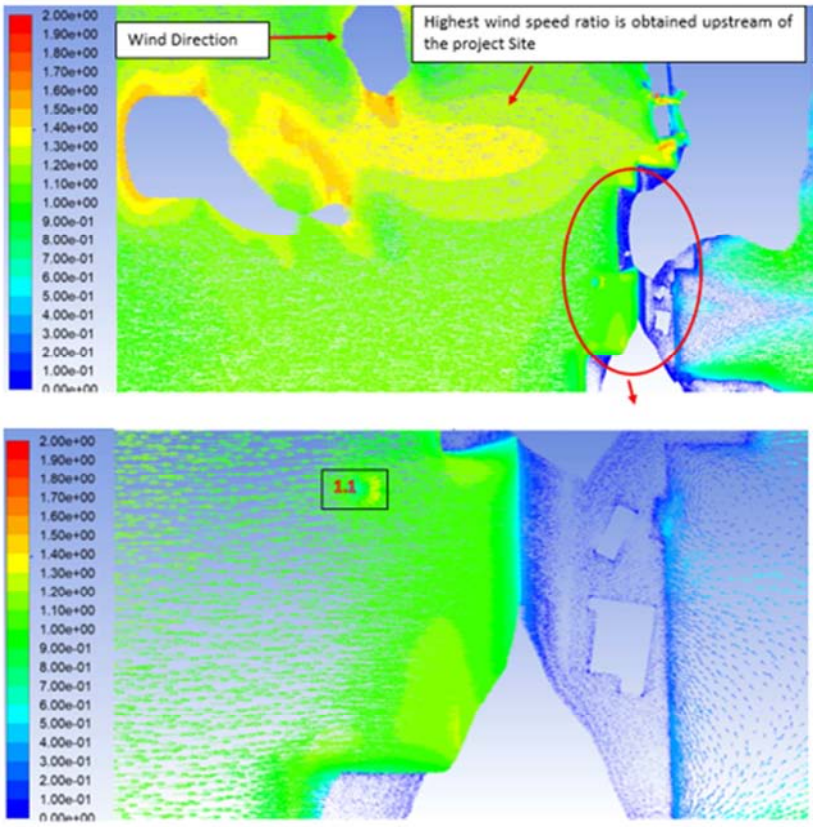

Figure 10. *Mean Velocity Ratios ($V_{local}/V_{reference}$ at 10m) Coloured by Velocity Vector – West Wind (15 m above the ground).*

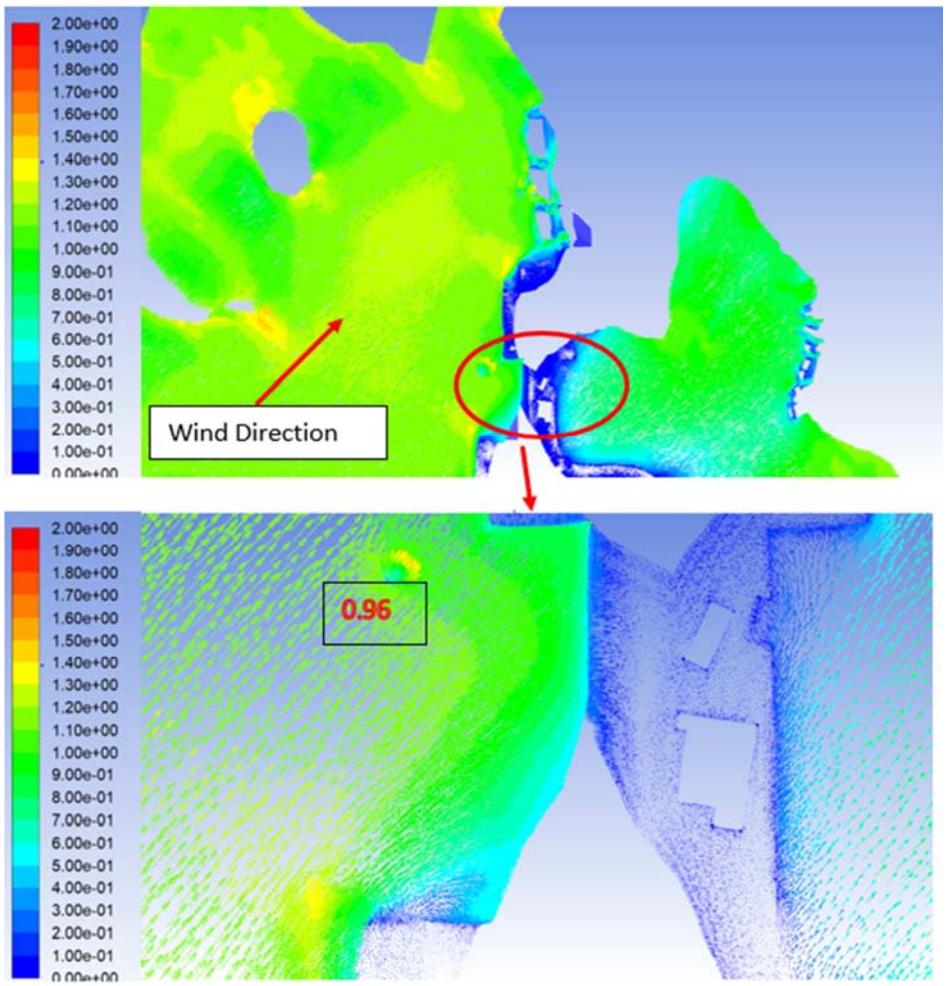

Figure 11. *Mean Velocity Ratios ($V_{local}/V_{reference}$ at 10m) Coloured by Velocity Vector – Southwest Wind (15 m above the ground).*

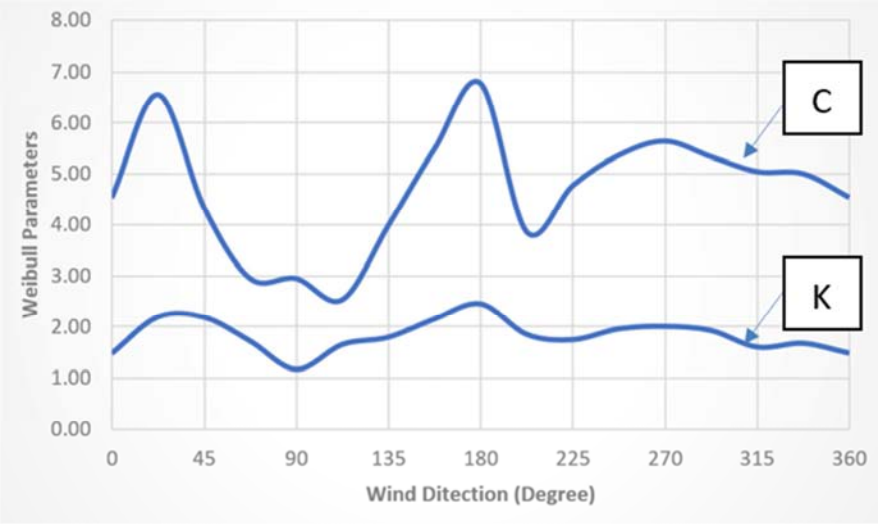

Figure 12. *Localised Weibull Parameters for 22.5° Band.*

4. Wind Energy

Wind power involves converting wind energy into electricity using wind turbines. A wind turbine is composed of propeller-like blades called rotors. The rotors are attached to the top of a tall tower. The tower usually comprises a tall mast (~15 m or higher) to take advantage of stronger winds away from the ground. The average wind speed needs to be above 5 m/s (18 km per hour) to make installing a wind turbine cost-competitive. Ideal locations for wind turbines are in rural areas, especially on elevated topography, or at the coast:

essentially, anywhere away from built-up areas with good exposure to oncoming winds from prevailing wind directions.

A typical wind turbine system configuration is shown in Figure 13 below:

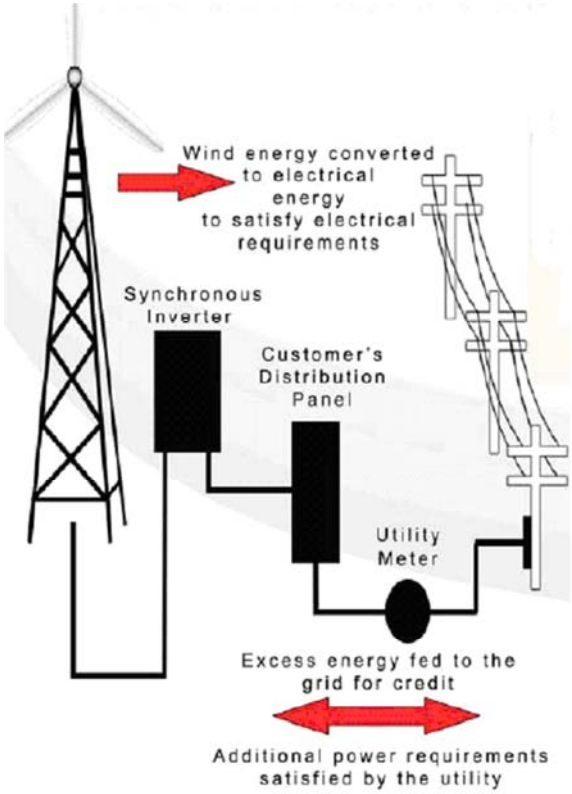

Figure 13. *Wind Turbine Systems Configurations.*

The wind resource is usually expressed as a wind speed or energy density, and typically, there will be a cut-off value below which the energy that can be extracted is insufficient to merit a wind energy development.

The wind analysis in this study was based on wind modelling for 8 wind directions.

The density function which can be used to describe the wind speed frequency curve using Weibull function is shown in Figure 14. The probability of the wind speed being equal to or greater than a specified wind speed, "u", is:

$$F(u)=1-\exp[-(u/C)^k]$$

From the above equation for example the probability that the wind speed is greater than or equal to 4 m/s is 44.2%, which implies:

$$(0.442*8760)=3{,}872 \text{ hours/year}$$

The wind speed is extremely important in terms of the amount of energy a wind turbine can convert to electricity; the wind power vs wind speed is shown in Figure 15. One can see that the power in 1 m^2 of wind with a speed of 5 m/s is 77 W while the power in the same 1 m^2 of area when the wind speed is 10 m/s is 613 W, therefore, if the wind speed doubles, it contains eight times as much energy.

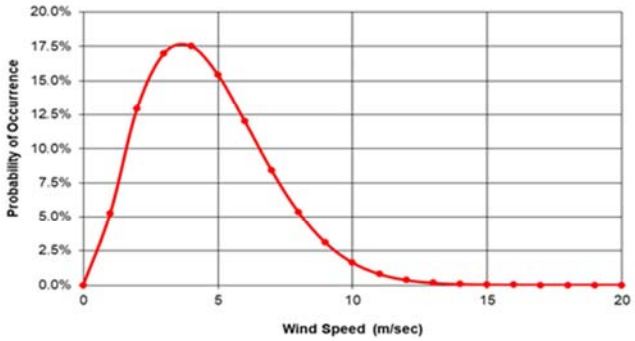

Figure 14. *Annual Wind Data and Weighted Weibull Density Function for the Proposed Site.*

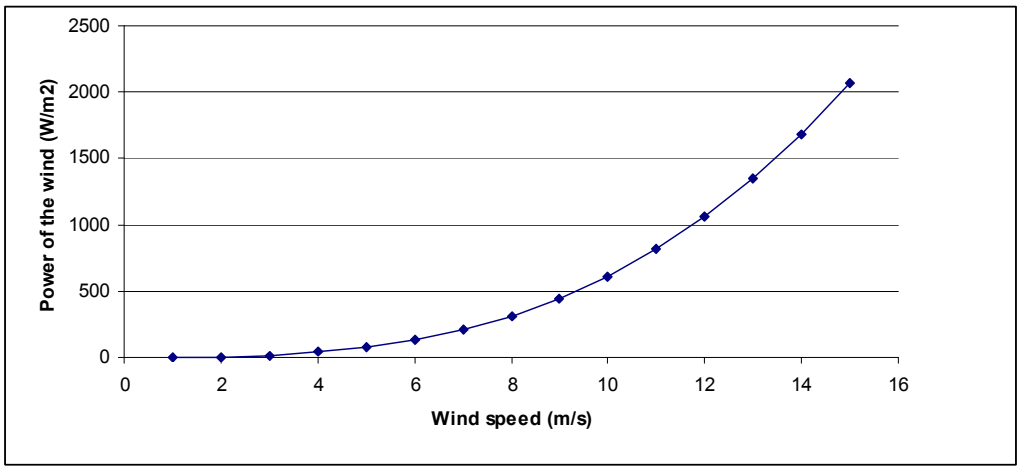

Figure 15. *Power of the Wind (W/m^2).*

The fraction of power extracted from the power in the wind by a particular wind turbine is usually given by a coefficient of performance, Cp:

$$P_{Turbine}=Cp * P_{wind}$$

The coefficient of performance is not constant, but varies with the wind speed, the rotational speed of the turbine and turbine blade parameters such as angle of attack and pitch angle.

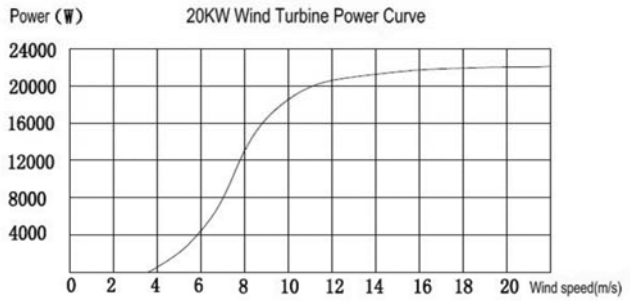

Figure 16. *20 kW Wind Turbine Power Curve.*

Technical data for urban wind turbines of different sizes and shapes can be obtained from turbine suppliers. An example of a manufacturer-provided power curve for a commercially available 20 kW horizontal wind turbine is shown in Figure 16.

The following comments are made regarding Figure 15:

1) Cut in speed is about 3 m/s and the cut-out speed is about 25 m/s.
2) 20 kW power output is achieved at a wind speed of about 11 m/s at the hub height.

Assuming the wind turbine hub is located at 15 m above ground and the above wind turbine selected, an annual output of 26,112 kWh may be obtained (See Figure 17). This figure assumes that the proposed wind turbine is operational and continuously available. In practice, however, wind turbines need servicing and inspection once a year to ensure that they remain safe. In addition, component failures and accidents (such as lightning strikes) may disable wind turbines. Reliable statistics show that the best turbine manufacturers consistently achieve availability factors above 98%.

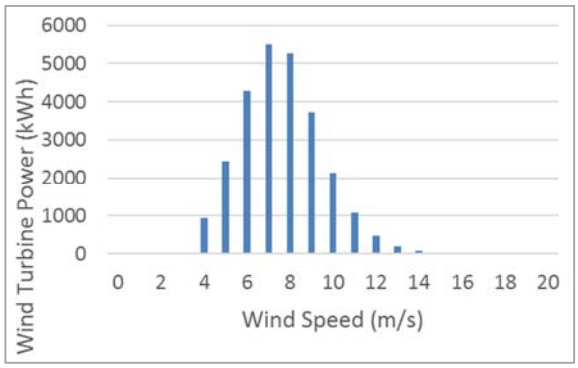

Figure 17. *Estimated Annual Power for the Proposed Site Using H9.0 Hammer WT 20kW.*

Maintenance and inspection works can be done during a calm wind condition when there is no power can be generated.

Wind power increases in height as does the wind speed. It is recommended that the hub of the tower is located at least 15 m above ground (10 m above any obstruction within 100-200 m radius).

5. Conclusions

A reliable integrated methodology and procedure is presented to:

1) Develop statistically reliable wind climate information for a Typical Meteorological Year (TMY), or more appropriately from long-term historical data from nearby weather stations.
2) Assess urban wind turbine feasibility using CFD analysis. CFD simulations of principal wind directions are used to establish an optimum wind turbine position.
3) Adjust the local statistical wind climate based on the CFD results for the proposed wind turbine location.
4) Estimate the annual wind power.
5) Optimize energy production where possible.

The CFD simulations in the current study accounted for complex site topography and incorporated the sheltering impact of nearby trees and other vegetation in order to find the least turbulent area for a successful installation.

The paper also discussed some of the parameters that have influence on the numerical results accuracy.

The CFD tool can also have multiple “downstream” applications, for example the same model could be used to model factors to be considered in the design of a micro-wind turbine (eg number of blades, shapes, etc.).

References

[1] Cace, J, Horst, E., Syngellakis, K, Niel, M., Clement, A., Heppener, R., Peiranon, E. (2007). Urban Wind Turbines Guidelines for Small Wind Turbines in the Built Environment, Intelligent Energy Europe.

[2] Wineur (2007). Urban Wind Turbines Technology Review: A text to the Catalogue of European Urban Wind Turbine Manufacturers, Intelligent Energy Europe, 1-9.

[3] NSW Small Wind Turbine Consumer Guide (2010). NSW Office of Environmental and Heritage, 1-73. https://www.environment.nsw.gov.au/resources/households/NSWSmallWindTurbineConsumerGuide.pdf.

[4] Warwick Wind Trials Project: Final Report (2009). Encraft Project, UK.

[5] Smith, J., Forsyth, T., Sinclair, K., Oteri, F. (2012). Built-Environment Wind Turbine Roadmap; Technical Report NREL/TP-5000-50499, National Renewable Energy Laboratory: Golden, CO, USA.

[6] Biswal, G., Shukla, S. (2015) Site Selection for Wind Farm Installation, IJIREEICE 3 (8), 2321-2004.

[7] Hymas, M. (2012). Wind Energy in the Built Environment, Metropolitan Sustainability, 457-499.

[8] Tian, L., Zhu, W., Shen, W., Zhao. N., Shen, Z. (2015). Development and Validation of a New two-dimensional Wake Model for Wind Turbines. Journal of Wind Engineering an Industrial Aerodynamics, 137, 90-99.

[9] Wind PRO (2017). Remote sensing data and other data for download in Wind PRO. Web: http://www.emd.dk/files/windpro/WindPRO_OnlineData.pdf

[10] Open wind (2017), Web: http://software.awstruepower.com/openwind.

[11] Bckmore, P. (2008). Siting Micro-Wind Turbines on House Roofs; IHS BRE Press: Watford, UK, 1–25.

[12] Blocken, B., Stathopoulos, T. (2013). CFD Simulation of Pedestrian-level Wind Conditions Around Buildings: Past Achievements and Prospects, International Journal of Wind Engineering & Industrial Aerodynamics, Editorial to Virtual Special Issue, 1-14.

[13] Franke, J., Hirsch, C., Jensen, A., Krüs, H., Schatzmann, M., Westbury, P., Miles, S., J. Wisse, N Wright N. (2004). Recommendations on the use of CFD in Wind Engineering, International Conference on Urban Wind Engineering and Building Aerodynamics (Ed. van Beeck JPAJ).

[14] Al-Khalidy, N. (2016). The Role of Computational Fluid Dynamics in Solving Wind Engineering Problems, IEEE Computer Society Conference Publishing Services, Crete, Greece, ISBN: 978-960-474-398-8, 109-116.

[15] Al-Khalidy, N. (2012). Designing Better Building with Computational Fluid Dynamics Analysis, 4th International Congress on Computational Engineering and Sciences, Las Vegas, University of Nevada, Reno, USA.

[16] Al-Khalidy, N. (2018) Building Generated Wind Shear and Turbulence Prediction utilising Computational Fluid Dynamics, WSEAS Transactions on Fluid Mechanics, 13, 126-135.

[17] Toja-Silva, Kono, T., Peralta, C., Lopez-Garcia, O., Chen, J. (2018). A review of computational fluid dynamics (CFD) simulations of the wind flow around buildings for urban wind energy exploitation, Journal of Wind Engineering and Industrial Aerodynamics, INDAER, 3675, 2018.

[18] Pierik, J., Dekker, J., Braam, H., Bulder, B., Winkelaar, D., Larsen, G., Morfiadakis, E., Chaviaropoulos, P., Derrick, A., Molly, J. (1999). Wind energy for the Next Millennium. In Proceedings of the European Wind Energy Conference, Nice, France, 1–5.

[19] Yang, A., Su, Y., Wen, C., Juan, Y., Wang, W., Chen, C. (2016) Estimation of Wind Power Generation in Dense Urban Area, Applied Energy, 171, 213-230.

[20] Lanzafame's Lab. (2019). Micro H-Darrieus Wind Turbines: CFD Modeling and Experimental Validation, AIP Conference Proceedings, DOI: 10.1063/1.5138842

[21] Kono, T., Kogaki, T., and Kiwata, T. (2016). Numerical Investigation of Wind Conditions for Roof-Mounted Wind Turbines: Effects of Wind Direction and Horizontal Aspect Ratio of a High-Rise Cuboid Building, Energies, 9, 907.

[22] Ansys Fluent Theory Manual (2019), ANSYS, USA.